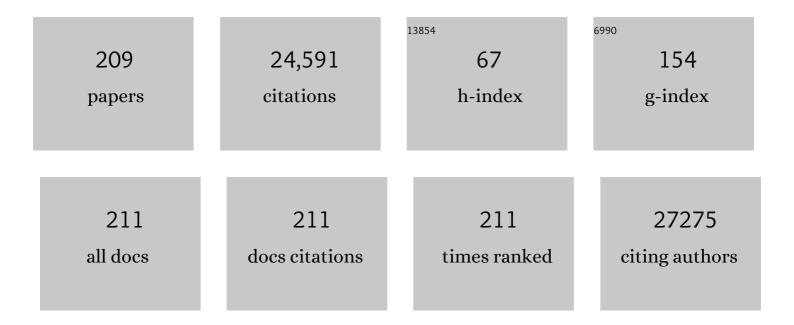
List of Publications by Year in descending order

Source: https://exaly.com/author-pdf/5418554/publications.pdf Version: 2024-02-01



Ζηένητα Νι

#	Article	IF	CITATIONS
1	Atomicâ€Layer Graphene as a Saturable Absorber for Ultrafast Pulsed Lasers. Advanced Functional Materials, 2009, 19, 3077-3083.	7.8	2,310
2	Uniaxial Strain on Graphene: Raman Spectroscopy Study and Band-Gap Opening. ACS Nano, 2008, 2, 2301-2305.	7.3	1,409
3	Raman spectroscopy and imaging of graphene. Nano Research, 2008, 1, 273-291.	5.8	1,181
4	Graphene Thickness Determination Using Reflection and Contrast Spectroscopy. Nano Letters, 2007, 7, 2758-2763.	4.5	1,034
5	Strong Photoluminescence Enhancement of MoS <sub>2</sub> through Defect Engineering and Oxygen Bonding. ACS Nano, 2014, 8, 5738-5745.	7.3	995
6	Broadband graphene polarizer. Nature Photonics, 2011, 5, 411-415.	15.6	961
7	Hopping transport through defect-induced localized states in molybdenum disulphide. Nature Communications, 2013, 4, 2642.	5.8	935
8	Two-dimensional antimonene single crystals grown by van der Waals epitaxy. Nature Communications, 2016, 7, 13352.	5.8	798
9	Raman Studies of Monolayer Graphene: The Substrate Effect. Journal of Physical Chemistry C, 2008, 112, 10637-10640.	1.5	663
10	Probing Layer Number and Stacking Order of Few‣ayer Graphene by Raman Spectroscopy. Small, 2010, 6, 195-200.	5.2	650
11	Plasma-assisted fabrication of monolayer phosphorene and its Raman characterization. Nano Research, 2014, 7, 853-859.	5.8	606
12	Two-dimensional transition metal dichalcogenides: interface and defect engineering. Chemical Society Reviews, 2018, 47, 3100-3128.	18.7	604
13	Raman spectroscopy of epitaxial graphene on a SiC substrate. Physical Review B, 2008, 77, .	1.1	477
14	Monolayer graphene as a saturable absorber in a mode-locked laser. Nano Research, 2011, 4, 297-307.	5.8	408
15	Layer-by-Layer Thinning of MoS <sub>2</sub> by Plasma. ACS Nano, 2013, 7, 4202-4209.	7.3	387
16	Plasmons in graphene: Recent progress and applications. Materials Science and Engineering Reports, 2013, 74, 351-376.	14.8	323
17	Broadband Photovoltaic Detectors Based on an Atomically Thin Heterostructure. Nano Letters, 2016, 16, 2254-2259.	4.5	322
18	Thickness-Dependent Reversible Hydrogenation of Graphene Layers. ACS Nano, 2009, 3, 1781-1788.	7.3	320

#	Article	IF	CITATIONS
19	Two-dimensional quasi-freestanding molecular crystals for high-performance organic field-effect transistors. Nature Communications, 2014, 5, 5162.	5.8	315
20	Tunable Stress and Controlled Thickness Modification in Graphene by Annealing. ACS Nano, 2008, 2, 1033-1039.	7.3	304
21	Interference enhancement of Raman signal of graphene. Applied Physics Letters, 2008, 92, .	1.5	292
22	High Responsivity Phototransistors Based on Few‣ayer ReS <sub>2</sub> for Weak Signal Detection. Advanced Functional Materials, 2016, 26, 1938-1944.	7.8	270
23	Raman Mapping Investigation of Graphene on Transparent Flexible Substrate: The Strain Effect. Journal of Physical Chemistry C, 2008, 112, 12602-12605.	1.5	260
24	On Resonant Scatterers As a Factor Limiting Carrier Mobility in Graphene. Nano Letters, 2010, 10, 3868-3872.	4.5	256
25	Reduction of Fermi velocity in folded graphene observed by resonance Raman spectroscopy. Physical Review B, 2008, 77, .	1.1	247
26	Evolution of Raman spectra in nitrogen doped graphene. Carbon, 2013, 61, 57-62.	5.4	228
27	Edge chirality determination of graphene by Raman spectroscopy. Applied Physics Letters, 2008, 93, .	1.5	226
28	Symmetry Breaking of Graphene Monolayers by Molecular Decoration. Physical Review Letters, 2009, 102, 135501.	2.9	224
29	Electronic structure of graphite oxide and thermally reduced graphite oxide. Carbon, 2011, 49, 1362-1366.	5.4	218
30	Highâ€Performance Monolayer WS <sub>2</sub> Fieldâ€Effect Transistors on Highâ€₽ Dielectrics. Advanced Materials, 2015, 27, 5230-5234.	11.1	218
31	The effect of vacuum annealing on graphene. Journal of Raman Spectroscopy, 2010, 41, 479-483.	1.2	216
32	The thermal stability of graphene in air investigated by Raman spectroscopy. Journal of Raman Spectroscopy, 2013, 44, 1018-1021.	1.2	209
33	Probing Charged Impurities in Suspended Graphene Using Raman Spectroscopy. ACS Nano, 2009, 3, 569-574.	7.3	196
34	High-performance siliconâ^'graphene hybrid plasmonic waveguide photodetectors beyond 1.55 μm. Light: Science and Applications, 2020, 9, 29.	7.7	155
35	FeCl <sub>3</sub> â€Based Fewâ€Layer Graphene Intercalation Compounds: Single Linear Dispersion Electronic Band Structure and Strong Charge Transfer Doping. Advanced Functional Materials, 2010, 20, 3504-3509.	7.8	154
36	High-performance graphene photodetector using interfacial gating. Optica, 2016, 3, 1066.	4.8	152

#	Article	IF	CITATIONS
37	Defect Engineering for Modulating the Trap States in 2D Photoconductors. Advanced Materials, 2018, 30, e1804332.	11.1	146
38	Stacking-Dependent Optical Conductivity of Bilayer Graphene. ACS Nano, 2010, 4, 4074-4080.	7.3	145
39	Engineering the Electronic Structure of Graphene. Advanced Materials, 2012, 24, 4055-4069.	11.1	141
40	Raman vibrational spectra of bulk to monolayer <mml:math xmlns:mml="http://www.w3.org/1998/Math/MathML"&gt;<mml:mrow><mml:mi>Re</mml:mi><mml:msub><mml:mi mathvariant="normal"&gt;S<mml:mn>2</mml:mn></mml:mi </mml:msub></mml:mrow>with lower symmetry. Physical Review B, 2015, 92, .</mml:math 	1.1	140
41	Ultrafast Growth of Highâ€Quality Monolayer WSe <sub>2</sub> on Au. Advanced Materials, 2017, 29, 1700990.	11.1	139
42	2D Singleâ€Crystalline Molecular Semiconductors with Precise Layer Definition Achieved by Floatingâ€Coffeeâ€Ringâ€Driven Assembly. Advanced Functional Materials, 2016, 26, 3191-3198.	7.8	136
43	Epitaxial Ultrathin Organic Crystals on Graphene for Highâ€Efficiency Phototransistors. Advanced Materials, 2016, 28, 5200-5205.	11.1	134
44	Raman spectroscopic investigation of carbon nanowalls. Journal of Chemical Physics, 2006, 124, 204703.	1.2	131
45	Room temperature ferromagnetism in partially hydrogenated epitaxial graphene. Applied Physics Letters, 2011, 98, .	1.5	126
46	Defects as a factor limiting carrier mobility in WSe2: A spectroscopic investigation. Nano Research, 2016, 9, 3622-3631.	5.8	126
47	Transition metal dichalcogenides bilayer single crystals by reverse-flow chemical vapor epitaxy. Nature Communications, 2019, 10, 598.	5.8	124
48	Flexible transformation plasmonics using graphene. Optics Express, 2013, 21, 10475.	1.7	117
49	<mml:math <br="" xmlns:mml="http://www.w3.org/1998/Math/MathML">display="inline"&gt;<mml:mi>G</mml:mi></mml:math> -band Raman double resonance in twisted bilayer graphene: Evidence of band splitting and folding. Physical Review B, 2009, 80, .	1.1	116
50	Biaxial Compressive Strain Engineering in Graphene/Boron Nitride Heterostructures. Scientific Reports, 2012, 2, 893.	1.6	113
51	Comparison of surface-enhanced Raman scattering on graphene oxide, reduced graphene oxide and graphene surfaces. Carbon, 2013, 62, 422-429.	5.4	107
52	Thickness identification of two-dimensional materials by optical imaging. Nanotechnology, 2012, 23, 495713.	1.3	101
53	Defect Engineering in 2D Materials: Precise Manipulation and Improved Functionalities. Research, 2019, 2019, 4641739.	2.8	101
54	Fabrication of Graphene Nanodisk Arrays Using Nanosphere Lithography. Journal of Physical Chemistry C, 2009, 113, 6529-6532.	1.5	98

#	Article	IF	CITATIONS
55	Defect-Engineered Heat Transport in Graphene: A Route to High Efficient Thermal Rectification. Scientific Reports, 2015, 5, 11962.	1.6	96
56	Electronic Structures and Structural Evolution of Hydrogenated Graphene Probed by Raman Spectroscopy. Journal of Physical Chemistry C, 2011, 115, 1422-1427.	1.5	95
57	Spectroscopic investigation of defects in two-dimensional materials. Nanophotonics, 2017, 6, 1219-1237.	2.9	94
58	Atomic-layer soft plasma etching of MoS2. Scientific Reports, 2016, 6, 19945.	1.6	93
59	Precise, Self-Limited Epitaxy of Ultrathin Organic Semiconductors and Heterojunctions Tailored by van der Waals Interactions. Nano Letters, 2016, 16, 3754-3759.	4.5	92
60	Improving the Performance of Graphene Phototransistors Using a Heterostructure as the Light-Absorbing Layer. Nano Letters, 2017, 17, 6391-6396.	4.5	87
61	Excitonic Dynamics in Janus MoSSe and WSSe Monolayers. Nano Letters, 2021, 21, 931-937.	4.5	86
62	Orientation-Dependent Raman Spectroscopy of Single Wurtzite CdS Nanowires. Journal of Physical Chemistry C, 2008, 112, 1865-1870.	1.5	83
63	Defect Activated Photoluminescence in WSe <sub>2</sub> Monolayer. Journal of Physical Chemistry C, 2017, 121, 12294-12299.	1.5	83
64	Gold on graphene as a substrate for surface enhanced Raman scattering study. Applied Physics Letters, 2010, 97, .	1.5	81
65	A van der Waals pn heterojunction with organic/inorganic semiconductors. Applied Physics Letters, 2015, 107, 183103.	1.5	77
66	Strong ferromagnetism of reduced graphene oxide. Carbon, 2014, 78, 559-565.	5.4	73
67	Direct determination of the crystallographic orientation of graphene edges by atomic resolution imaging. Applied Physics Letters, 2010, 97, 053110.	1.5	70
68	Lowâ€Temperature Eutectic Synthesis of PtTe <sub>2</sub> with Weak Antilocalization and Controlled Layer Thinning. Advanced Functional Materials, 2018, 28, 1803746.	7.8	70
69	Probing the intrinsic optical quality of CVD grown MoS2. Nano Research, 2017, 10, 1608-1617.	5.8	67
70	High-performance position-sensitive detector based on graphene–silicon heterojunction. Optica, 2018, 5, 27.	4.8	63
71	Isolating hydrogen in hexagonal boron nitride bubbles by a plasma treatment. Nature Communications, 2019, 10, 2815.	5.8	63
72	Strong optical response and light emission from a monolayer molecular crystal. Nature Communications, 2019, 10, 5589.	5.8	59

#	Article	IF	CITATIONS
73	Graphene Surface Plasmon Induced Optical Field Confinement and Lasing Enhancement in ZnO Whispering-Gallery Microcavity. ACS Applied Materials & Interfaces, 2014, 6, 10469-10475.	4.0	54
74	Graphene-Based Infrared Position-Sensitive Detector for Precise Measurements and High-Speed Trajectory Tracking. Nano Letters, 2019, 19, 8132-8137.	4.5	52
75	Visibility study of graphene multilayer structures. Journal of Applied Physics, 2008, 103, .	1.1	51
76	Thermal Dynamics of Graphene Edges Investigated by Polarized Raman Spectroscopy. ACS Nano, 2011, 5, 147-152.	7.3	51
77	Shape-Uniform, High-Quality Monolayered MoS <sub>2</sub> Crystals for Gate-Tunable Photoluminescence. ACS Applied Materials & Interfaces, 2017, 9, 42121-42130.	4.0	51
78	How defects influence the photoluminescence of TMDCs. Nano Research, 2021, 14, 29-39.	5.8	51
79	Improving the electrical performance of MoS <sub>2</sub> by mild oxygen plasma treatment. Journal Physics D: Applied Physics, 2017, 50, 154001.	1.3	50
80	Fabrication of sub-nanometer pores on graphene membrane for ion selective transport. Nanoscale, 2018, 10, 5350-5357.	2.8	50
81	Graphene Sheet-Induced Global Maturation of Cardiomyocytes Derived from Human Induced Pluripotent Stem Cells. ACS Applied Materials & Interfaces, 2017, 9, 25929-25940.	4.0	48
82	Gateâ€Tunable Polar Optical Phonon to Piezoelectric Scattering in Few‣ayer Bi <sub>2</sub> O <sub>2</sub> Se for Highâ€Performance Thermoelectrics. Advanced Materials, 2021, 33, e2004786.	11.1	48
83	Fast Photoelectric Conversion in the Nearâ€Infrared Enabled by Plasmonâ€Induced Hotâ€Electron Transfer. Advanced Materials, 2019, 31, e1903829.	11.1	44
84	Determination of Raman Phonon Strain Shift Coefficient of Strained Silicon and Strained SiGe. Japanese Journal of Applied Physics, 2005, 44, 7922-7924.	0.8	42
85	Anisotropy of electron-phonon coupling in single wurtzite CdS nanowires. Applied Physics Letters, 2007, 91, .	1.5	41
86	High output mode-locked laser empowered by defect regulation in 2D Bi2O2Se saturable absorber. Nature Communications, 2022, 13, .	5.8	41
87	SERS-active ZnO/Ag hybrid WGM microcavity for ultrasensitive dopamine detection. Applied Physics Letters, 2016, 109, .	1.5	40
88	High pressure photoluminescence and Raman investigations of CdSeâ^•ZnS core/shell quantum dots. Applied Physics Letters, 2007, 90, 021921.	1.5	38
89	High-rate, low-temperature synthesis of composition controlled hydrogenated amorphous silicon carbide films in low-frequency inductively coupled plasmas. Journal Physics D: Applied Physics, 2008, 41, 055406.	1.3	38
90	Electronic transport and layer engineering in multilayer graphene structures. Applied Physics Letters, 2008, 92, .	1.5	37

#	Article	IF	CITATIONS
91	Low temperature edge dynamics of AB-stacked bilayer graphene: Naturally favored closed zigzag edges. Scientific Reports, 2011, 1, 12.	1.6	37
92	Graphene plasmon guided along a nanoribbon coupled with a nanoring. Journal Physics D: Applied Physics, 2014, 47, 135106.	1.3	37
93	Molybdenum Oxide/Tungsten Oxide Nano-heterojunction with Improved Surface-Enhanced Raman Scattering Performance. ACS Applied Materials & Interfaces, 2021, 13, 33345-33353.	4.0	37
94	Heat conduction across metal and nonmetal interface containing imbedded graphene layers. Carbon, 2013, 64, 61-66.	5.4	36
95	Sulfurâ€Mastery: Precise Synthesis of 2D Transition Metal Dichalcogenides. Advanced Functional Materials, 2019, 29, 1809261.	7.8	36
96	2D atomic crystal molecular superlattices by soft plasma intercalation. Nature Communications, 2020, 11, 5960.	5.8	36
97	Characterization of graphene layers using super resolution polarization parameter indirect microscopic imaging. Optics Express, 2014, 22, 20446.	1.7	34
98	High temperature Raman spectroscopy studies of carbon nanowalls. Journal of Raman Spectroscopy, 2007, 38, 1449-1453.	1.2	32
99	Highly efficient broadband photodetectors based on lithography-free Au/Bi <sub>2</sub> O <sub>2</sub> Se/Au heterostructures. Nanoscale, 2019, 11, 20707-20714.	2.8	32
100	Bi2O2Se/BP van der Waals heterojunction for high performance broadband photodetector. Science China Information Sciences, 2021, 64, 1.	2.7	31
101	Realization of vertical and lateral van der Waals heterojunctions using two-dimensional layered organic semiconductors. Nano Research, 2017, 10, 1336-1344.	5.8	30
102	The effect of graphene on surface plasmon resonance of metal nanoparticles. Physical Chemistry Chemical Physics, 2018, 20, 25078-25084.	1.3	29
103	Soft hydrogen plasma induced phase transition in monolayer and few-layer MoTe <sub>2</sub> . Nanotechnology, 2019, 30, 034004.	1.3	29
104	Ultrafast carrier dynamics in pristine and FeCl3-intercalated bilayer graphene. Applied Physics Letters, 2010, 97, 141910.	1.5	28
105	Thermal transport and energy dissipation in two-dimensional Bi2O2Se. Applied Physics Letters, 2019, 115, .	1.5	28
106	Vis-NIR photodetector with microsecond response enabled by 2D bismuth/Si(111) heterojunction. 2D Materials, 2021, 8, 035002.	2.0	27
107	Stimulated emission of CdS nanowires grown by thermal evaporation. Applied Physics Letters, 2007, 91,	1.5	26
108	Organic charge-transfer interface enhanced graphene hybrid phototransistors. Organic Electronics, 2019, 64, 22-26.	1.4	25

#	Article	IF	CITATIONS
109	The influence of chemical solvents on the properties of CVD graphene. Journal of Raman Spectroscopy, 2015, 46, 21-24.	1.2	24
110	Electron contributions to the heat conduction across Au/graphene/Au interfaces. Carbon, 2017, 115, 665-671.	5.4	24
111	Producing air-stable InSe nanosheet through mild oxygen plasma treatment. Semiconductor Science and Technology, 2018, 33, 074002.	1.0	24
112	Ultrasonic exfoliated ReS <sub>2</sub> nanosheets: fabrication and use as co-catalyst for enhancing photocatalytic efficiency of TiO <sub>2</sub> nanoparticles under sunlight. Nanotechnology, 2019, 30, 184001.	1.3	24
113	Raman mapping investigation of chemical vapor deposition-fabricated twisted bilayer graphene with irregular grains. Physical Chemistry Chemical Physics, 2014, 16, 21682-21687.	1.3	23
114	Synergistic graphene/aluminum surface plasmon coupling for zinc oxide lasing improvement. Nano Research, 2017, 10, 1996-2004.	5.8	23
115	Controllable Synthesis of Crystalline ReS <sub>2(1â<sup>^*</sup></sub> <i><sub>x</sub></i> <sub>)</sub> Se <sub>2</sub> <i><sub>x</sub></i> Monolayers on Amorphous SiO <sub>2</sub> /Si Substrates with Fast Photoresponse. Advanced Optical Materials, 2020. 8. 1901415.	3.6	23
116	Lattice dynamics in monolayer and few-layer SnSe2. Physical Review B, 2017, 96, .	1.1	22
117	Zn doped MAPbBr <sub>3</sub> single crystal with advanced structural and optical stability achieved by strain compensation. Nanoscale, 2020, 12, 3692-3700.	2.8	22
118	MoS <sub>2</sub> /WSe <sub>2</sub> vdW Heterostructures Decorated with PbS Quantum Dots for the Development of High-Performance Photovoltaic and Broadband Photodiodes. ACS Nano, 2022, 16, 9329-9338.	7.3	22
119	Bandgapâ€Opened Bilayer Graphene Approached by Asymmetrical Intercalation of Trilayer Graphene. Small, 2015, 11, 1177-1182.	5.2	21
120	Plasmon–phonon coupling in monolayer WS2. Applied Physics Letters, 2016, 108, .	1.5	21
121	Surface modification of all-inorganic halide perovskite nanorods by a microscale hydrophobic zeolite for stable and sensitive laser humidity sensing. Nanoscale, 2020, 12, 13360-13367.	2.8	21
122	Effect of the surface oxide layer on the stability of black phosphorus. Applied Surface Science, 2021, 537, 147850.	3.1	21
123	Fourfold Polarization‣ensitive Photodetector Based on GaTe/MoS <sub>2</sub> van der Waals Heterojunction. Advanced Electronic Materials, 2022, 8, 2100673.	2.6	21
124	Surface enhanced Raman scattering of aged graphene: Effects of annealing in vacuum. Applied Physics Letters, 2011, 99, .	1.5	20
125	Ultrasensitive grapheneâ€5i positionâ€sensitive detector for motion tracking. InformaÄnÃ-Materiály, 2020, 2, 761-768.	8.5	20
126	Surface-enhanced Raman scattering from graphene covered gold nanocap arrays. Journal of Applied Physics, 2013, 114, .	1.1	19

#	Article	IF	CITATIONS
127	Patterning Graphene Film by Magnetic-assisted UV Ozonation. Scientific Reports, 2017, 7, 46583.	1.6	19
128	Luminescence signature of free exciton dissociation and liberated electron transfer across the junction of graphene/GaN hybrid structure. Scientific Reports, 2015, 5, 7687.	1.6	18
129	Janus Monolayers for Ultrafast and Directional Charge Transfer in Transition Metal Dichalcogenide Heterostructures. ACS Nano, 2022, 16, 4197-4205.	7.3	18
130	Large-size Mo1-xWxS2 and W1-xMoxS2 (x = 0–0.5) monolayers by confined-space chemical vapor deposition. Applied Surface Science, 2018, 457, 591-597.	3.1	17
131	Surface-Enhanced Raman Scattering Monitoring of Oxidation States in Defect-Engineered Two-Dimensional Transition Metal Dichalcogenides. Journal of Physical Chemistry Letters, 2020, 11, 7981-7987.	2.1	17
132	High-pressure Raman and photoluminescence of highly anisotropic CdS nanowires. Journal of Raman Spectroscopy, 2007, 38, 1112-1116.	1.2	16
133	Fluorescence quenching of CdSe quantum dots on graphene. Applied Physics Letters, 2013, 103, 201909.	1.5	16
134	Thickness-Dependent Interlayer Charge Transfer in MoSe <sub>2</sub> /MoS <sub>2</sub> Heterostructures Studied by Femtosecond Transient Absorption Measurements. ACS Applied Materials & Interfaces, 2021, 13, 6489-6495.	4.0	16
135	The dispersion of graphene in conductive epoxy composites investigated by Raman spectroscopy. Journal of Raman Spectroscopy, 2017, 48, 432-436.	1.2	15
136	Visualization and investigation of Si–C covalent bonding of single carbon nanotube grown on silicon substrate. Applied Physics Letters, 2008, 93, 103111.	1.5	14
137	Thickness and stacking geometry effects on high frequency overtone and combination Raman modes of graphene. Journal of Raman Spectroscopy, 2013, 44, 86-91.	1.2	14
138	Manipulating fluorescence quenching efficiency of graphene by defect engineering. Applied Physics Express, 2016, 9, 055502.	1.1	14
139	Position-sensitive detectors based on two-dimensional materials. Nano Research, 2021, 14, 1889-1900.	5.8	14
140	MnO2/Au hybrid nanowall film for high-performance surface-enhanced Raman scattering substrate. Applied Surface Science, 2015, 333, 78-85.	3.1	13
141	Controlling phase transition in WSe2 towards ideal n-type transistor. Nano Research, 2021, 14, 2703-2710.	5.8	13
142	Sub-4 nm Nanodiamonds from Graphene-Oxide and Nitrated Polycyclic Aromatic Hydrocarbons at 423 K. ACS Nano, 2021, 15, 17392-17400.	7.3	13
143	Defect-related dynamics of photoexcited carriers in 2D transition metal dichalcogenides. Physical Chemistry Chemical Physics, 2021, 23, 8222-8235.	1.3	13
144	Optical and Field Emission Properties of Zinc Oxide Nanostructures. Journal of Nanoscience and Nanotechnology, 2005, 5, 1683-1687.	0.9	12

#	Article	IF	CITATIONS
145	Broadband subwavelength imaging using non-resonant metamaterials. Applied Physics Letters, 2014, 104, 073502.	1.5	12
146	High-Performance Graphene-Based Electrostatic Field Sensor. IEEE Electron Device Letters, 2017, 38, 1136-1138.	2.2	12
147	Nonvolatile Memory Based on Molecular Ferroelectric/Graphene Field Effect Transistor. ACS Applied Materials & Interfaces, 2018, 10, 39187-39193.	4.0	11
148	Thickness-dependent enhanced optoelectronic performance of surface charge transfer-doped ReS2 photodetectors. Nano Research, 2022, 15, 3638-3646.	5.8	11
149	Confocal white light reflection imaging for characterization of metal nanostructures. Optics Communications, 2008, 281, 5360-5363.	1.0	10
150	Comment on "Raman spectra of misoriented bilayer graphene― Physical Review B, 2009, 79, .	1.1	10
151	Band-Bending at the Graphene–SiC Interfaces: Effect of the Substrate. Japanese Journal of Applied Physics, 2010, 49, 01AH05.	0.8	10
152	Distinct photoresponse in graphene induced by laser irradiation. Applied Physics Letters, 2015, 106, .	1.5	10
153	Determination of the thickness of two-dimensional transition-metal dichalcogenide by the Raman intensity of the substrate. Materials Research Express, 2016, 3, 025007.	0.8	10
154	Defect engineering in two-dimensional materials. Journal of Semiconductors, 2019, 40, 070403.	2.0	10
155	Raman spectra evidence for the covalent-like quasi-bonding between exfoliated MoS2 and Au films. Science China Information Sciences, 2021, 64, 1.	2.7	10
156	Enhancement of weak localization for nitrogen-doped graphene by short range potentials. Carbon, 2015, 82, 346-352.	5.4	9
157	Investigation of dodecane in three-dimensional porous graphene sponge by Raman mapping. Nanotechnology, 2016, 27, 055702.	1.3	9
158	Controllable n-type doping in WSe2 monolayer via construction of anion vacancies. Chinese Chemical Letters, 2021, 32, 3118-3122.	4.8	9
159	Phase Transition Mechanism in KIO3Single Crystals. Journal of Physics: Conference Series, 2006, 28, 105-109.	0.3	8
160	Investigation of multilayer domains in large-scale CVD monolayer graphene by optical imaging. Journal of Semiconductors, 2017, 38, 033003.	2.0	8
161	Photoluminescence characterization of the grain boundary thermal stability in chemical vapor deposition grown WS <sub>2</sub> . Materials Research Express, 2017, 4, 106202.	0.8	8
162	Making few-layer graphene photoluminescent by UV ozonation. Optical Materials Express, 2016, 6, 3527.	1.6	7

#	Article	IF	CITATIONS
163	Raman spectroscopy study of twisted tetralayer graphene. Journal of Raman Spectroscopy, 2016, 47, 668-673.	1.2	7
164	Excitonic Emission in Atomically Thin Electroluminescent Devices. Laser and Photonics Reviews, 2021, 15, 2000587.	4.4	7
165	Tunable self-trapped excitons in 2D layered rubrene. Applied Physics Letters, 2021, 118, .	1.5	7
166	The Thinnest Light Disk: Rewritable Data Storage and Encryption on WS <sub>2</sub> Monolayers. Advanced Functional Materials, 2021, 31, 2103140.	7.8	7
167	Synthesis of Single- and Few-Layer Nitrogen-doped Graphene and Layer-Dependent Surface-Enhanced Raman Scattering Properties. Journal of Physical Chemistry C, 2021, 125, 17831-17840.	1.5	7
168	Spectroscopic Perception of Trap States on the Performance of Methylammonium and Formamidinium Lead Iodide Perovskite Solar Cells. Advanced Materials, 2021, 33, 2102241.	11.1	7
169	Plasmonâ€enhanced polarized Raman spectroscopy for sensitive surface characterization. Journal of Raman Spectroscopy, 2008, 39, 1338-1342.	1.2	6
170	Strong room-temperature blue-violet photoluminescence of multiferroic BaMnF <sub>4</sub> . Physical Chemistry Chemical Physics, 2016, 18, 2054-2058.	1.3	6
171	Optical studies of the thermal stability of InSe nanosheets. Applied Surface Science, 2019, 467-468, 860-867.	3.1	6
172	High pressure photoluminescence and Raman studies of ZnxCd1â^'xSe quantum dots. Journal of Physics Condensed Matter, 2008, 20, 325214.	0.7	5
173	Metal Hydroxide and Metal Oxide Nanostructures from Metal Corrosion. Journal of Nanoscience and Nanotechnology, 2009, 9, 1496-1500.	0.9	5
174	Selectively enhanced Raman scattering with triple-resonance nanohole arrays. Optics Communications, 2019, 452, 494-498.	1.0	5
175	UV Rewritable Hybrid Graphene/Phosphor p–n Junction Photodiode. ACS Applied Materials & Interfaces, 2019, 11, 43351-43358.	4.0	5
176	Competition between Oxygen Curing and Ion Migration in MAPbI <sub>3</sub> Induced by Irradiation Exposure. Journal of Physical Chemistry Letters, 2020, 11, 8477-8482.	2.1	5
177	Optoelectronic performance of multilayer WSe <sub>2</sub> transistors enhanced by defect engineering. Applied Physics Express, 2020, 13, 061004.	1.1	5
178	Bidirectional doping of two-dimensional thin-layer transition metal dichalcogenides using soft ammonia plasma. Nanoscale, 2021, 13, 15278-15284.	2.8	5
179	Correlated Dynamics of Free and Selfâ€Trapped Excitons and Broadband Photodetection in BEA <sub>2</sub> PbBr <sub>4</sub> Layered Crystals. Advanced Optical Materials, 2022, 10, .	3.6	5
180	Optical and Magnetic Properties of Ni-Doped ZnO Nanocones. Journal of Nanoscience and Nanotechnology, 2007, 7, 3620-3623.	0.9	4

#	Article	IF	CITATIONS
181	Synthesis, Optical, and Magnetic Properties of Ba <sub>2</sub> Ni <sub>3</sub> F <sub>10</sub> Nanowires. ACS Applied Materials & Interfaces, 2016, 8, 26213-26219.	4.0	4
182	Ultrasensitive graphene position-sensitive detector induced by synergistic effects of charge injection and interfacial gating. Nanophotonics, 2020, 9, 2531-2536.	2.9	4
183	Strong Green Luminescence of Mg-Doped ZnO Nanowires. Journal of Nanoscience and Nanotechnology, 2006, 6, 2529-2532.	0.9	3
184	A Simple Route to Growth of Silicon Nanowires. Journal of Nanoscience and Nanotechnology, 2008, 8, 5787-5790.	0.9	3
185	Exploring the working mechanism of graphene patterning by magnetic-assisted UV ozonation. Physical Chemistry Chemical Physics, 2017, 19, 27353-27359.	1.3	3
186	Photoinduced doping in monolayer WSe <sub>2</sub> transistors. Applied Physics Express, 2019, 12, 094005.	1.1	3
187	Surface-Related Exciton and Lasing in CdS Nanostructures. Nanoscale Research Letters, 2019, 14, 216.	3.1	3
188	Thermally enhanced optical contrast of graphene oxide for thickness identification. Nanotechnology, 2019, 30, 295704.	1.3	3
189	Achieving high-performance multilayer MoSe <sub>2</sub> photodetectors by defect engineering*. Chinese Physics B, 2021, 30, 087801.	0.7	3
190	Tunable anisotropy in ReS2 flakes achieved by Ar+ ion bombardment probed by polarized Raman spectroscopy. Applied Physics Letters, 2021, 119, 053104.	1.5	3
191	Potassium lodide Doping Strategy for High-Efficiency Perovskite Solar Cells Revealed by Ultrafast Spectroscopy. Journal of Physical Chemistry Letters, 2022, 13, 711-717.	2.1	3
192	Resonance Raman scattering on graded-composition W <i>x</i> Mo1– <i>x</i> S2 alloy with tunable excitons. Applied Physics Letters, 2022, 120, .	1.5	3
193	Raman Enhancement Caused by Gold Nanoparticles Clustered Between Graphene and Substrate. Journal of Nanoscience and Nanotechnology, 2015, 15, 3173-3177.	0.9	2
194	Modulation of THz radiation via enhanced Dirac plasmon-dual phonon interaction. Applied Physics Letters, 2019, 115, .	1.5	2
195	Photoluminesence enhancement at high generation rate induced by exciton localization. Optics Letters, 2021, 46, 2774-2777.	1.7	2
196	The phase transition in PrGa0.95Mg0.05O3 at elevated temperatures. Journal of Physics and Chemistry of Solids, 2009, 70, 533-535.	1.9	1
197	Thermoelectric Materials: Gateâ€Tunable Polar Optical Phonon to Piezoelectric Scattering in Fewâ€Layer Bi <sub>2</sub> O <sub>2</sub> Se for Highâ€Performance Thermoelectrics (Adv. Mater. 4/2021). Advanced Materials, 2021, 33, 2170023.	11.1	1
198	The Thinnest Light Disk: Rewritable Data Storage and Encryption on WS <sub>2</sub> Monolayers (Adv.) Tj ETQ	2q0_0_0 rgE	3T /Overlock 1

#	Article	IF	CITATIONS
199	Suppression of Surface Defects and Vibrational Coupling in GaN by a Graphene Monolayer. Physica Status Solidi - Rapid Research Letters, 2022, 16, 2100489.	1.2	1
200	Lithography-free and high-efficiency preparation of black phosphorous devices by direct evaporation through shadow mask. Nanotechnology, 2022, 33, 225201.	1.3	1
201	Disorder induced bands in first order Raman spectra of carbon nanowalls. , 0, , .		0
202	Disorder induced bands in first order Raman spectra of carbon nanowalls. , 2006, , .		0
203	Modifying Properties of Grapheneâ $\in$ "a Raman Microscopic Study. , 2010, , .		0
204	Stacking dependent optical properties of bilayer graphene. , 2010, , .		0
205	A Mild and Efficient Transfer Method of Two-dimensional Materials for the Third Generation DNA Sequencing. , 2015, , .		0
206	Manipulating fluorescence intensity with mechanical strains. Materials Research Express, 2015, 2, 015017.	0.8	0
207	Enhanced stimulated brillouin scattering effect by using multilayer molybdenum disulfide on fibre end. , 2017, , .		0
208	Raman Imaging of Two Dimensional Materials. Springer Series in Materials Science, 2019, , 231-261.	0.4	0
209	Aggregationâ€Dependent Dielectric Permittivity in 2D Molecular Crystals. Small Methods, 2022, , 2101198.	4.6	0